7.4.   Evaluation of Slope Stability

7.4.1.   Method of Slope Stability Evaluation

(1) Present Topographic Condition and Slope Stability Condition

Kutay Özaydın (2001) summarized the general conditions of slopes as follows:

> In areas where the surface geology is of Güngören or Gülpnar Formations, many landslides occur. This sliding phenomenon is characteristic of areas with the following: 1) ground surface gradient exceeds 30%, 2) cut and fill work are undertaken, and 3) a change of groundwater level occurs.

Erdoğan Yüzer (2001) summarized the general condition of slopes as follows:

> On the Asian side, surface geology is mainly rock, and landslides are not common. On the European side, landslides are observed alongside coast lines and their adjacent areas. This phenomena is observed far beyond the Silivri District. The scale of the slide can be from 50 m to several hundred meters of sliding blocks of soil. The eastside slope of Büyükçekmece Lake, the south coast of the Avcılar District, and southwest coast of Küçükçekmece lake are especially typical landslide areas. In these areas, soil strength is considered as a residual condition.

The JICA Study team also observed some surface failures of slope in rock formations. In these areas the slope gradient was observed as over 100%, and there are residential buildings in below and atop failure surfaces.

Considering the above mentioned slope conditions, major types of slope failure are classified as follows:

Area of Rock Formation

> Rock formation slope failure takes into account the surface failure of weathered zones or talus. Large rock failures, exceeding several hundreds meters, are not considered. Stability of these kinds of large failures must be examined through detailed and individual investigations.

Area of Tertiary Formation

> Güngören Formation and Gülpnar Formation areas have often suffered from landslide activities. Ground strength is considered a residual condition. Surface failure of weathered zones or talus is considered in other areas characterized prevailingly by Tertiary deposits.

Area of Quaternary Formation and Fill Material

General circular slip is considered.

(2) Method of the Slope Stability Evaluation

Siyahi and Ansal studied a procedure of slope stability for microzonation purposes. This procedure is introduced in the "Manual for Zonation on Seismic Geotechnical Hazards" by TC4, ISSMFE (1993). Applicability of the procedure was validated against an earthquake that occurred in 1967 affecting the Akyokus Village, in the Adapazarı region of Turkey. Bilge Siyahi (1998) revised this procedure. Variation in shear strength with depth is assumed, and potential failure surface is taken as a circular arc. Finally, a safety factor *Fs* for slope stability is induced as

$$Fs = N_1 \tan \phi \qquad \text{(eq.7.4.1)}$$
where N_1: stability number
ϕ: angle of internal friction

Thus, the safety factor depends on the angle of shear strength and stability number N_1 representing the configuration of the slope and failure surface. The minimum value of the stability number is determined by carrying out a parametric study on configuration of slope and N to find the most critical failure surface as given in Figure 7.4.1. The variation of minimum N_1 can be expressed as a function of β (slope angle) and A (earthquake acceleration). It becomes possible to calculate the minimum safety factor Fs, if ϕ value can be determined or estimated.
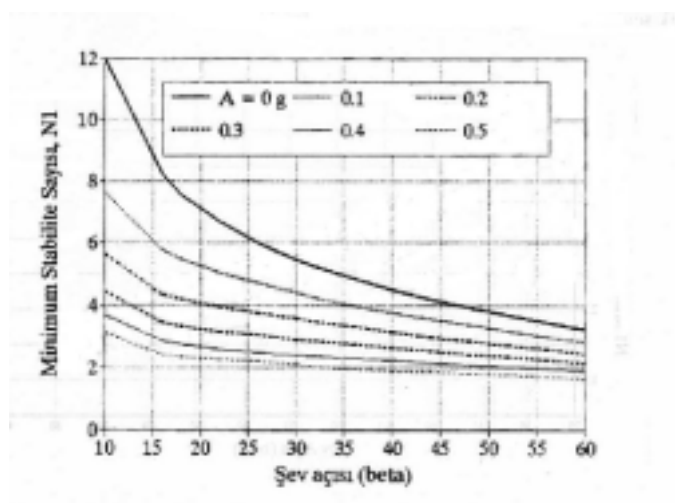
Horizontal axis:	Slope gradient (degree)
Vertical axis:	Minimum shear strength stability index
A:	Acceleration
g:	Gravitational acceleration

Figure 7.4.1   Relationship between Slope Gradient, Seismic Coefficient and Minimum Shear Strength Stability Number

Source: Siyahi (1998)

(3) Consideration of Analysis Procedure

There are varieties of slope characteristics in the Study Area, thus, it is difficult to identify slope failure parameters for every slope in detail. Therefore, it is required that slope stability be qualitatively evaluated, assuming slope failure categorization.

Siyahi's procedure introduced the idea for obtaining minimum safety factors for various shapes of failure surface and slope. It also assumes circular arc failure in normally consolidated soil. Slope gradient and shear strength are the only required data for calculation.

Furthermore, as results of the parametric approach, this procedure is considered to extend to not only circular surface failure, but, to some extent, another type of slope failure. Slopes and failure types in the Study Area are not always that assumed in Siyahi's procedure. However, the characteristics of the procedure act advantageously in considering the slope failure categorization.

In this Study, Siyahi's procedure is applied to evaluate slope stability for small analysis units. Each result of evaluations is aggregated into microzonation units.

(4) Procedure of Analysis and Evaluation of Stability

The outline of the evaluation method is described below and shown in Figure 7.4.2.
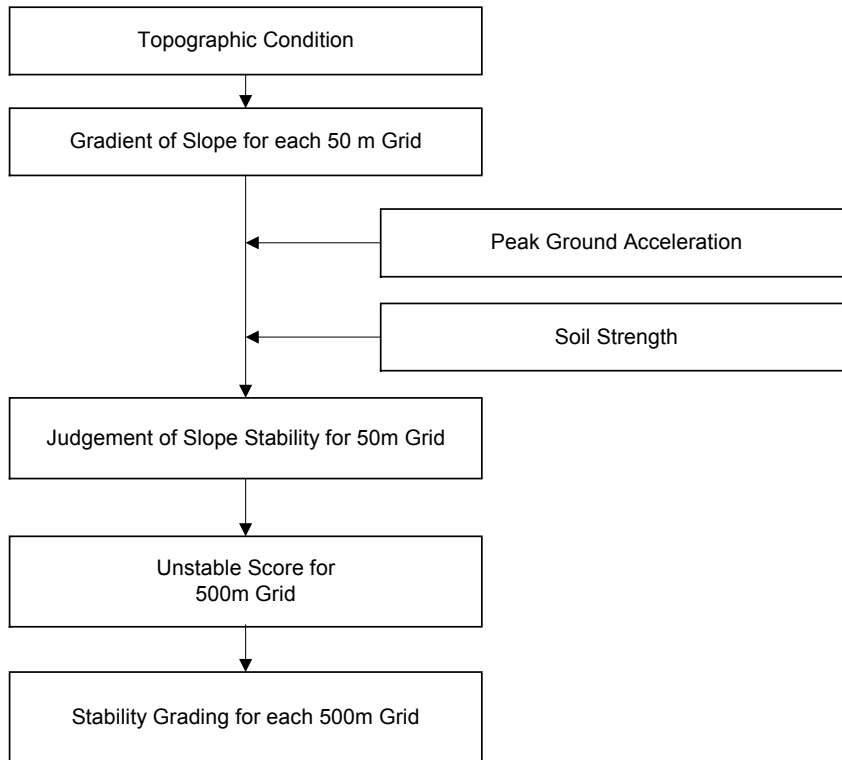
Figure 7.4.2   Flowchart of Slope Failure Evaluation

Source: The JICA Study Team

a.   Slope Stability Evaluation for 50 m Grids

The slope gradient for each 50 m gri, that covers all of the Study Area is calculated first. Then, the slope stability of each point is judged using Siyahi's equation (Eqn. 7.4.1), taking the peak ground acceleration value and strength of soil into account. A score $F_i = 0$ for a stable point (Fs > 1.0) or $F_i = 1$ for an unstable point (Fs < 1.0) is then given.

b.   Slope Stability Evaluation for 500 m Grids

There are a total 100 of 50 m-grids in every 500 m grid, and the stability score for each 500 m grid is determined as follows:

$$\text{Unstable Score}\,(500\text{m Grid}) = \sum_{i=1}^{100} \text{Score}\, F_i\,(50\text{m Grid})$$

$$F_i\,(50\text{m Grid}) = 1\,(unstable) \quad or \quad 0\,(stable)$$

If all 50 m grids are evaluated as unstable, then *Score (500m grid)* is calculated as 100. If all 50 m grids are evaluated as stable, then *Score (500m grid)* is calculated as 0. This score

directly represents what percent of the 50 m grids in each 500 m grid is judged as unstable. Finally, the results are represented by risk for each 500 m grid, as shown in Table 7.4.1.

Table 7.4.1   Evaluation of Risks on Slope Stability for 500m Grid

Unstable Score (500m Grid)	Risk Evaluation for 500m Grid
0	Very low
1-30	Low
31-60	High
61-100	Very high

(5) Parameters for Calculation

a. Slope Gradient

Slope gradient is determined as 50 m grid base.

b. Ground Motion

Scenario Earthquake Model A and model C are considered because these two scenarios represent the most general hazard conditions.

c. Shear Strength of Ground

Shear strength is the most important parameter for calculation. Available data on shear strength for soil is limited and does not cover all the geological formations. Therefore, values are estimated considering two existing references. One is *strength of sliding surface for weathered rocks*, quoted in   "Design Guideline for Road Construction, Slope Treatments and Stabilization," Japan Road Association, 1999.   Another reference is *strength of sliding surface for weathered rocks*, quoted in "Slope Stability and Stabilization Methods," L. Abramson et al., 1996.   The determined strength of each formation and considered failure type are summarized in Table 7.4.2.
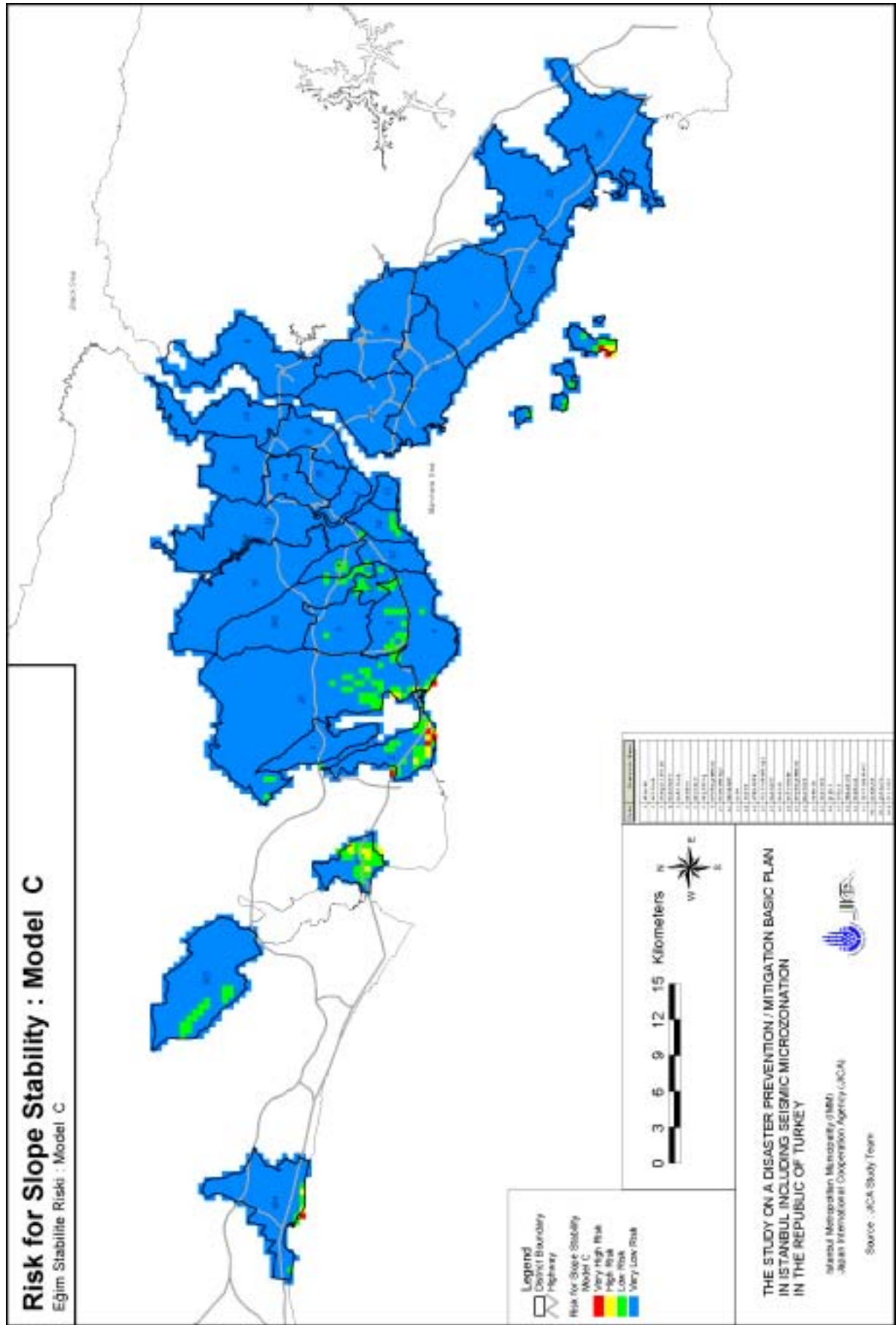
Table 7.4.2   Applied Angle of Shear Strength for Slope Stability Calculation

Ground Type	Geological Formation		Angle of Shear Strength (Degree)	Remarks
	Geological Map	Formation		
Rock	IMM 1:5,000	Kuf, Af, Gf, Df, Kf, Tf, Blf, Trf, Bg, V	25	Considering surface failure of weathered zone or talus.
	MP 1:50,000	Kuf, Af, Gf, Df, Kf, Tf, Blf, Trf, Kz, Saf		
	MTA 1:25,000	tsk, ts, tq, ptq		
Tertiary Sediments	IMM 1:5,000	Sf, Cf, Baf	25	Considering surface failure of weathered zone or talus.
	MP 1:50,000	Sf, Cf, Baf		
	IMM 1:5,000	Cmlf	15	Same as Güf, Gnf
	IMM 1:5,000	Sbf, Çf, Saf	30	Considering surface failure of weathered zones or talus. Gravel conditions are taken into account.
	MP 1:50,000	Çf,		
	MTA 1:25,000	m2m3-19-k		
	IMM 1:5,000	Güf , Gnf	15	Landslides occur in these formations. Residual strength is considered.
	MP 1:50,000	Güf , Gnf		
	MTA 1:25,000	e3-ol1-10-s, ebed-20-s, ebed-8-s, m3-pl-18k, ol2-18-k, ol2m1-19-k, ol-8-s,pgg		
Quaternary Sediments	IMM 1:5,000	Ksf, Qal, Ym	25	General slope failure. Same as weathered zone.
	MP 1:50,000	Oa, Q		
	MTA 1:25,000	Q-21-k		
Fill	IMM 1:5,000	Yd, Sd	25	

Source: The JICA Study Team

7.4.2.   Slope Stability

(1) Slope Stability Risk

The results of the slope stability risk evaluation are shown in Figure 7.4.3 and Figure 7.4.4.

In the case of Model A, "very high risk" grids exist in Adalar and Silivri. These correspond to steep cliffs and not residential areas. "low risk" grids exist in Avcılar and Küçükçekmece, Büyükçekmece. These correspond to residential areas.

In the case of Model C, "very high risk" grids extend to Avcılar. "High risk" grids prevail in Büyükçekmece. These correspond to residential areas. "Low risk" grids extend through Bahçelievler, Bakirköy, and Güngören, and these correspond to residential areas.

Figure 7.4.3   Slope Stability Risk: Model A

Figure 7.4.4   Slope Stability Risk: Model C

(2) Slope Stability Condition for each District and Geological Formation Unit

Slope risks are examined on a more detailed level. Unstable scores are summarized for each district and each geological formation.

The stability score for each district is determined as follows:

$$\text{Unstable Score (District)} = \frac{\text{Number of Unstable 50m grid}}{\text{Number of 50m grid in the District}} \times 100 \, (\%)$$

First, slope stability for each 50 m grid is calculated. Next, the number of unstable grids in a district is calculated. Then, the area ratio for these grids is calculated. This score directly represents what percent of area for each district is unstable.

The stability score for each geological unit is determined as follows:

$$\text{Unstable Score (Geological Formation)} = \frac{\text{Number of Unstable 50m grid}}{\text{Number of 50m grid in the Formation}} \times 100 \, (\%)$$

First, slope stability for each 50 m grid is calculated. Next, the number of unstable grids in each geological formation is calculated. Then, the area ratio for these grids is calculated. This score directly represents what percent of area for each geological formation is unstable.

Unstable scores are summarized for each district and for geological formation units. Results are shown in Table 7.4.3 and Table 7.4.4, respectively.

In the Büyükçekmece District, areas of "low risk" and "high risk" prevail. Unstable scores are about 3% for Model A and about 7% for Model C, respectively. This area is characterized by landslides. Unstable areas are concentrated to the eastside slope of Büyükçekmece Lake. The low strength of the Güf Formation contributes to the resulting high damage ratio, even though the slope gradient is not steep.

In the Adalar District, areas of "high risk" and "very high risk" exist in the southern part of Büyükada Island. The area is closest to the source fault. Unstable scores are about 2% for Model A and about 5% for Model C, respectively. Unstable areas are concentrated on Büyükada Island because this district is closest to earthquake source fault.

In the Avcılar District, areas of "high risk" and "very high risk" exist in the southern part of the district. Unstable scores are about 1% for Model A and about 4% for Model C, respectively. This area is also characterized by landslides. Unstable areas are concentrated

in the southern coast area where Gnf formations prevail. Some unstable areas exist in the districts of Bahçelievler, Bakirköy, Güngören, Çatalca and Silivri.

Table 7.4.3   Results of Slope Stability Analysis by District

District Name	Calculation Points (50m grid)	Model A		Model C	
		Unstable Points (50m grid)	Unstable Score (Average Unstable Area Ratio %)	Unstable Points (50m grid)	Unstable Score (Average Unstable Area Ratio %)
Adalar	3786	75	1.98	185	4.89
Avcilar	15358	140	0.91	608	3.96
Bahçelievler	6638	26	0.39	111	1.67
Bakirköy	11678	49	0.42	95	0.81
Bağcilar	8768	0	0.00	8	0.09
Beykoz	15208	0	0.00	0	0.00
Beyoğlu	3487	0	0.00	0	0.00
Beşiktaş	7217	0	0.00	0	0.00
Büyükçekmece	5520	166	3.01	402	7.28
Bayrampaşa	3840	1	0.03	14	0.36
Eminönü	2001	0	0.00	0	0.00
Eyüp	20208	0	0.00	1	0.00
Fatih	4157	3	0.07	23	0.55
Güngören	2880	6	0.21	24	0.83
Gaziosmanpaşa	22680	0	0.00	0	0.00
Kadiköy	16304	0	0.00	0	0.00
Kartal	12462	0	0.00	0	0.00
Kağithane	5778	0	0.00	0	0.00
Küçükçekmece	47949	59	0.12	256	0.53
Maltepe	22038	0	0.00	0	0.00
Pendik	18822	0	0.00	0	0.00
Sariyer	11040	0	0.00	0	0.00
Şişli	14161	0	0.00	0	0.00
Tuzla	19641	0	0.00	0	0.00
Ümraniye	18252	0	0.00	0	0.00
Üsküdar	15059	0	0.00	0	0.00
Zeytinburnu	4583	0	0.00	2	0.04
Esenler	15552	0	0.00	16	0.10
Çatalca	21054	50	0.24	144	0.68
Silivri	15262	116	0.76	141	0.92
Total	391383	691	0.18	2030	0.52

Source: The JICA Study Team

Table 7.4.4   Results of Slope Stability Analysis by Geological Formation Unit

Covering Geological Map	Formation Name	Calculation Points (50m grid)	Model A		Model C	
			Unstable Points (50m grid)	Unstable Score (Average Unstable Ratio %)	Unstable Points (50m grid)	Unstable Score (Average Unstable Ratio %)
IMM 1:5,000 MP 1:50,000	Gnf	18562	259	1.59	1063	6.69
	Çmlf	3284	1	0.03	18	0.55
	Güf	1991	24	1.21	77	3.87
	Tf	2104	3	0.14	3	0.14
	Af	4497	52	1.16	144	3.20
	Kuf	24427	16	0.07	31	0.13
	V	436	4	0.92	7	1.61
MTA 1:25,000	ebed-8-s	908	25	2.75	73	8.04
	ol2-18-k	19289	282	1.46	544	2.82
	ol-8-s	488	24	4.92	60	12.30
	pgg	1026	1	0.10	10	0.97
Total		391383	691	0.18	2030	0.52

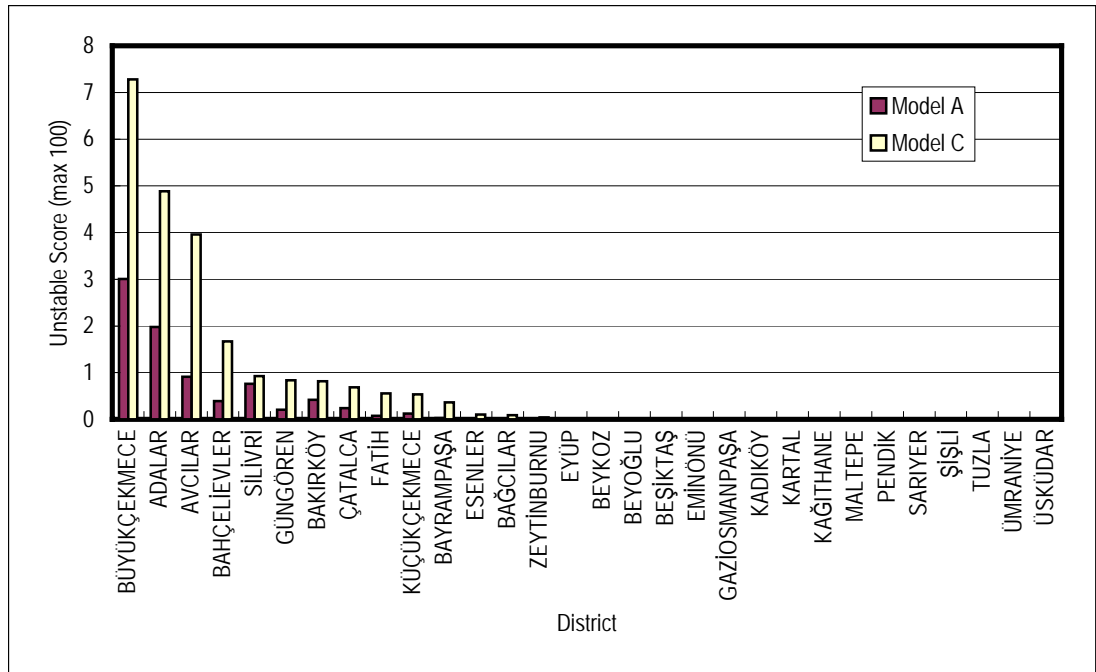Source: The JICA Study Team

Figure 7.4.5   Unstable Score (Area Ratio) of Slope by District
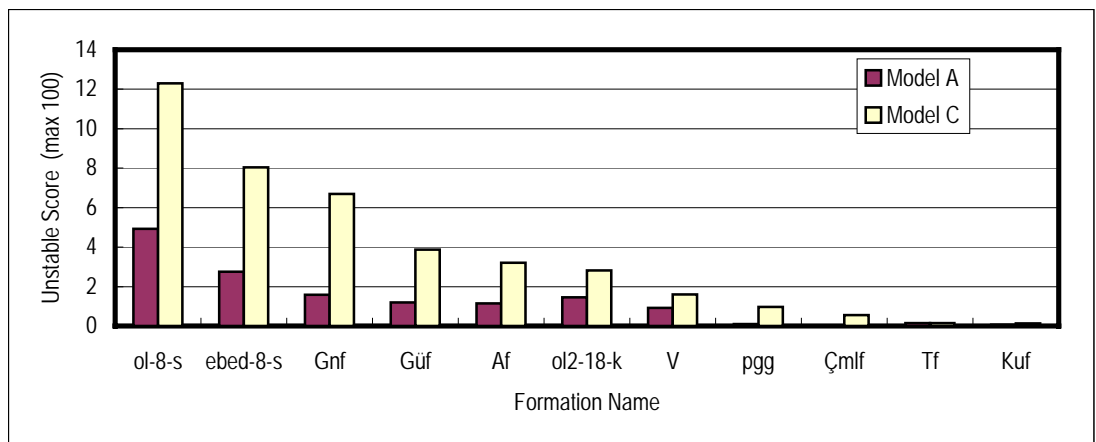
Souce: The JICA Study Team

Figure 7.4.6   Unstable Score (Area Ratio) of Slope by Geological Formation

Souce: The JICA Study Team

Acknowledgement

The slope stability analysis in this chapter was conducted under close discussions with Dr. Prof. Kutay Özaydın, Yıldız Technical University, Faculty of Civil Engineering, Department of Engineering, Geotechnical Division, Dr. Prof. Erdoğan Yüzer, Istanbul Technical University, Faculty of Mining, Geological Engineering Department, Dr. Assoc. Prof. Bilge G. Siyahi, Boğaziçi University, Kandilli Observatory and Earthquake Research Institute, and Department of Earthquake Engineering. The Study Team expresses special thanks to their collaboration.

References for Section 7.4

Bilge G. Siyahi, 1998, Deprem Etkısindeki Normal Konsolide Zemin Şevlerinde Yari-Statik Stabilite Analizi, İMO Teknik Dergi, Yazı 112, 1525-1552.

Erdoğan Yüzer, 2001, Privarte Interview.

ISSMFE, 1993, Manual for Zonation on Seismic Geotechnical Hazards, Technical Committee for Earthquake Geotechnical Engineering, TC4, International Society of Soil Mechanics and Foundation Engineering.

Japan Road Association, 1996, Japanese Design Specification of Highway Bridge (in Japanese).

Japan Road Association, 1999, Design Guideline for Road Construction, Slope Treatments and Stabilization, pp. 352. (in Japanese)

Kutay Özaydın, 2001, Private Interview.

Lee Abramson, Tom Lee, Suil Sharma, Glenn Boyce, 1996, Slope Stability and Stabilization Methods, John Willy & Sons, pp94.

Chapter 8.
Estimation of Damages and Casualties

Chapter 8.   Estimation of Damages and Casualties

Earthquake damage is calculated for Model A and Model C scenario earthquakes, respectively. Comparing the results of the seismic motion distribution of the four different scenario earthquakes shown in Chapter 7, the following observations can be made:

−   Distribution of peak ground acceleration (PGA) of Model D resembles that of Model A.

−   Therefore, the damage distribution pattern for Model D is expected to resemble to that of Model A.

−   PGA value of Model D is less than that of Model A. Therefore, damage for Model D will be less than that for Model A. On the European side, distribution of peak ground acceleration (PGA) of Model B is almost similar to that of Model C.

−   Therefore, the damage distribution pattern for Model B is expected to resemble to that of Model C.

−   PGA value of Model B is less than that of Model C.

−   Therefore, damage amount of Model B will be less than that of Model C.

To conclude, the damage estimation for Model A is conducted as the most probable case, and for Model C as the worst case.

Caution

Seismic microzonation is not the prophecy of future earthquakes. Scenario earthquakes are never meant predict the next event. It cannot be said that one of these models will occur next.

Though the analysis is based on up-to-date scientific knowledge, results include inevitable errors. The estimated damage amount and distribution included in this report can be used only for the purpose of establishing a disaster prevention / mitigation plan in Istanbul.

8.1. Buildings

8.1.1. Methodology

(1) General

a. Schematic Flow of Damage Estimation

In this study damage is estimated comparing **"the response displacement of the building"** and **"the displacement in which the building come at the damage"**. Schematic flow chart is shown in Figure 8.1.1.

Regarding **"the response displacement of the building"**;

The earthquake excitation can be given as **"Acceleration Response Spectrum S_a"**.

Each building is classified to the building type that is shown in Table 8.1.1, and kinetic modeling is carried out. **"Capacity Spectrum"** is established as a result.

"Response Displacement of Building" can be obtained using **"Acceleration Response Spectrum S_a"** and **"Capacity Spectrum"**.

In above-mentioned procedure, **"Capacity Spectrum"** is set taking account into the non-linearity caused by yielding of particular member of the building. Therefore **"Response Displacement of Building"** can be more certain index than acceleration or force. This is an advantage that can be obtained by using this method.

Regarding **"the displacement in which the building come at the damage"**;

The damage state is classified into 3 categories "Heavily" "Moderately" and "Partly" as shown in. Each damage state is defined by the value of story drift. Each value of story drift is converted into spectral displacement. However if the technological uncertainty of the earthquake motion and the building model is taken into account, a kind of probabilistic method is needed here because the damage state evaluation may have some dispersion. The lognormal distribution is applied in order to reflect this dispersion, and **"Fragility Function"** is obtained as a result. **"Fragility Function"** gives **"Damage Ratio"** that the building come at.

"Number of Damaged Buildings" can be obtained when **"Damage Ratio"** is multiplied by the number of buildings that is counted in **"Building Inventory"**.

Building damages are calculated based on scenario earthquakes Model A and Model C. In these estimations, every type of building included in the building census for the year 2000

is included. Important public facilities such as schools, hospitals, and fire stations will be studied separately in another chapter.

Buildings are calculated as "heavily," "moderately," or "partly" damaged. "Heavily" damaged buildings are buildings that are severely damaged or have collapsed, and these buildings are unfit to occupy until they are repaired or rebuilt. "Moderately" damaged buildings are buildings that are able to used for evacuation purposes just after the hazard, but they need to be repaired before occupied permanently. "Partly" damaged buildings can be used for living, but it is desirable they be repaired because the structure is partly damaged and its earthquake-resistance has been compromised.

The cause of damage is limited to the seismic vibration itself. Damage due to other causes such as liquefaction, landslide, and fire are not included. This assumption will not affect the result because these phenomena are not main causes of earthquake disasters in Istanbul.

Figure 8.1.1   Schematic Flowchart of Building Damage Estimation

b. **Building inventory for damage estimation**

In this study, building types are classified as shown in Table 8.1.1. Each group of building type is defined as a combination of "Structure", "Floor Number" and "Construction Year". The damage vulnerability function will be given for each of building type.

Table 8.1.1   Building Number by Classification for Damage Estimation

Classification	Structure	Floor Number	Construction Year			Total
			-1959	1960 - 1969	1970 -	
1	RC Frame with Brick Wall	1 - 3F	7,120 (1.0%)	13,757 (1.9%)	200,950 (27.7%)	221,827 (30.6%)
2		4 - 7F	6,280 (0.9%)	15,449 (2.1%)	280,231 (38.7%)	301,961 (41.7%)
3		8F -	481 (0.1%)	886 (0.1%)	18,468 (2.5%)	19,835 (2.7%)
4	Wood Frame	1 - 2F	4,755 (0.7%)	697 (0.1%)	1,583 (0.2%)	7,035 (1.0%)
5		3F -	3,611 (0.5%)	222 (0.0%)	358 (0.0%)	4,191 (0.6%)
6	RC Shear Wall	1 - 3F	1 (0.0%)	0 (0.0%)	13 (0.0%)	13 (0.0%)
7		4 - 7F	0 (0.0%)	0 (0.0%)	200 (0.0%)	200 (0.0%)
8		8F -	0 (0.0%)	0 (0.0%)	564 (0.1%)	564 (0.1%)
9	Masonry	1 - 2F	25,967 (3.6%)	24,881 (3.4%)	83,215 (11.5%)	134,063 (18.5%)
10		3F -	16,952 (2.3%)	8,208 (1.1%)	8,877 (1.2%)	34,037 (4.7%)
11	Prefabricated		20 (0.0%)	12 (0.0%)	864 (0.1%)	896 (0.1%)
Total			65,188 (9.0%)	64,113 (8.8%)	595,322 (82.2%)	724,623 (100.0%)

(2) Modeling and Capacity Spectrum

a. Modeling

Multi degree of freedom model (hereinafter referred to as "MDOFM"), that is shown schematically in Figure 8.1.2 is generated for each building type. Then a set of eigenvalue (natural period and eigen vector) is obtained applying eigenvalue analysis.

Single degree of freedom model (hereinafter reffered to as "SDOFM") can be substituted for MDOFM applying a set of eigenvalue. Response Displacement of Building S_d can be calculated using SDOFM.
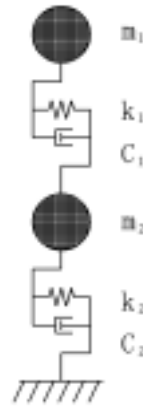
Figure 8.1.2   Schematic drawing of multi degree of freedom model (Example for 2 stories building)

b. Capacity Spectrum

The capacity Spectrum is configured using fundamental eigenvalue that is obtained by the procedure explained above. The concept of capacity Spectrum is shown in Figure 8.1.3.
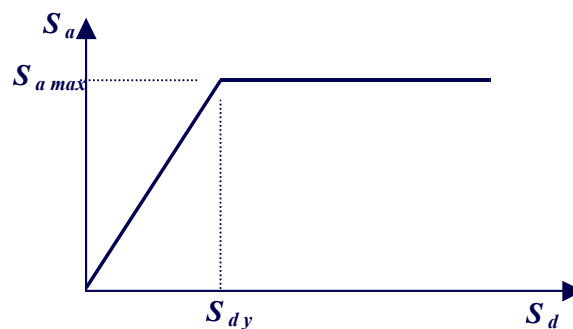

Figure 8.1.3   Schematic Drawing of Capacity Spectrum

Capacity spectrum defines a specific SDOFM that represents the component of fundamental eigenvalue of MDOFM explained in Figure 8.1.2.

Vertical axis of Fig. 8.1.3 shows the response acceleration that represents the component of fundamental eigenvalue of MDOFM S_a.   The horizontal axis shows the response displacement that represents the component of fundamental eigenvalue of MDOFM S_d.

Gradient of the second solid line in Figure 8.1.3 is assumed as horizontal. The off-set value of $(S_a)_{max}$ is given by Eq. (8.1.1).

$$(S_a)_{max} = \left(\frac{V}{W}\right)\frac{G}{\alpha_1}$$
(8.1.1)

where,

$(S_a)_{max}$ Capacity acceleration

$\left(\dfrac{V}{W}\right)$ Ratio of horizontal seismic load to weight

G Acceleration of gravity

α_1 Effective mass ratio of fundamental mode

$$\alpha_1 = \frac{M_{x1}}{\sum m_n} \tag{8.1.2}$$

where,

M_{x1} Effective mass of fundamental mode

$\sum m_n$ Total mass

Gradient of first solid line in Fig.8.1.3 represents the fundamental period, and is given by Eq. (8.1.3).

$$\frac{S_{a\,max}}{S_{d\,y}} = \left(\frac{2\pi}{T}\right)^2 \tag{8.1.3}$$

(3) Probabilistic Method and Fragility Function

a. Probabilistic Method

In this study, damage evaluation will be carried out using a fragility function that is given as a lognormal distribution in which a spectral displacement is applied as a stochastic variable. A basic equation is shown in Eq. (8.1.4).

$$P[D \geq d_s S_d] = \Phi\left[\frac{\ln\left(\dfrac{S_d}{S_{d,d_s}}\right)}{\beta_{ds}}\right] \tag{8.1.4}$$

where

$P[D \geq d_s S_d]$ Damage Ratio   It means probability of that damage state of the building D become under d_s.

S_d Spectral displacement

S_{d,d_s} Median values of spectral displacement when the building shows the damage state d_s

β_{ds} Standard deviation of logarithm of the displacement when the building shows the damage state d_s

Φ Operational calculus for obtaining the cumulative standard normal distribution functions

b. Fragility Function

The fragility function is to derive the relation between the damage ratio and response of building model. That is specified by the median values of spectral displacement when the building shows the each damage state S_{d,d_s} and Standard deviation of logarithm of the displacement when the building shows the each damage state β_{ds}. (See Eq. (8.1.4))

The value S_{d,d_s} is given by Eq. (8.1.5) on the basis of a story drift ratio D_s.

$$S_{d,d_s} = \frac{D_s}{F_p \left[\dfrac{\phi_j - \phi_{j+1}}{H_j} \right]_{max}} \qquad (8.1.5)$$

where,

D_s Story drift ratio when the damage state reaches d_s

F_p Participation Factor

ϕ_j Eigen vector of story j

H_j Height of story j

The remaining coefficient β_{ds} represents the dispersion of the value S_d. The coefficient of variation C_V that is defined in Eq. (8.1.6) and (8.1.7) is effective in determining the value β_{ds}.

$$\beta_{ds} = \sqrt{\ln \frac{1 + \sqrt{1 + 4\left(\dfrac{\sigma}{\exp\left(\ln S_{d,d_s}\right)} \right)^2}}{2}} \qquad (8.1.6)$$

$$\sigma = C_V \ S_{d,d_s} \qquad (8.1.7)$$

where

σ variance

C_V coefficient of variation

(4) Parameter setting

Several coefficients shall be determined to specify the capacity spectrum and the fragility function.   These coefficients are determined originally from building structure and individual from the seismic ground motion. It is an advantage of the damage estimation method employed in the Study that we can study the characteristics of the building and seismic ground motion separately.

At the initial stage of determination of the coefficients, the following items are taken into consideration.

1) Existing study on capacity of structure

2) Trend of earthquake resistant standard in the Study area

3) General common sense of construction engineer in the Study area

4) Impression from site survey in the Study area (especially, quality of finishing)

Actual dameges by past earthquakes also give convincing information. In other word, these can be regarded as actual size experiment. Therefore, those coefficients which are primarily determined are cariblated and reconsidered with reference to the existing past earthquake damage ratio. The coefficients are finally determined by following procedure.

1) Determine the coefficients temporarily based on descriptions in the earthquake resistant standard adopted in Istanbul, taking the result of site survey into consideration

2) Set the capacity spectrum and the fragility function and apply them to the area where the damages of past earthquake are reported

3) Applied seismic motion is the response spectrum accerelation calculated based on observed accerelation wave form which is considered to represent the actual seismic motion well.

4) Relations between Damage ratio and Seismic intensity are generally reported in those past earthquake damage investigations.   In this case, adjusted response spectrum accrelation at each building points are calculated from reported seismic intensities.

a. Capacity spectrum

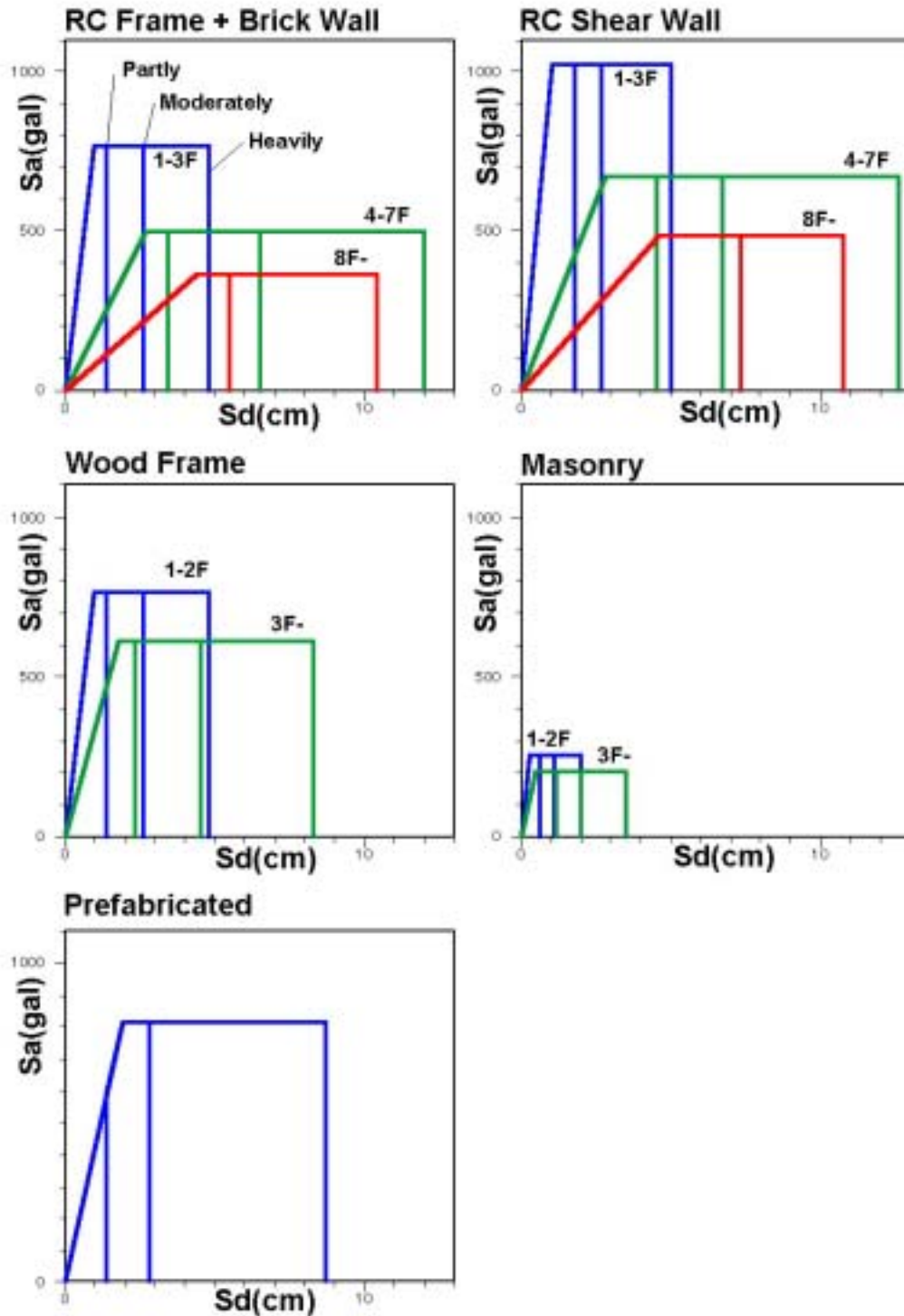Examples of capacity spectrum is shown in Figure 8.1.4.

Figure 8.1.4   Capacity Spectrum of the Buildings Constructed after 1970

b.   Fragility Function

Examples of fragility function are shown in Figure 8.1.5.
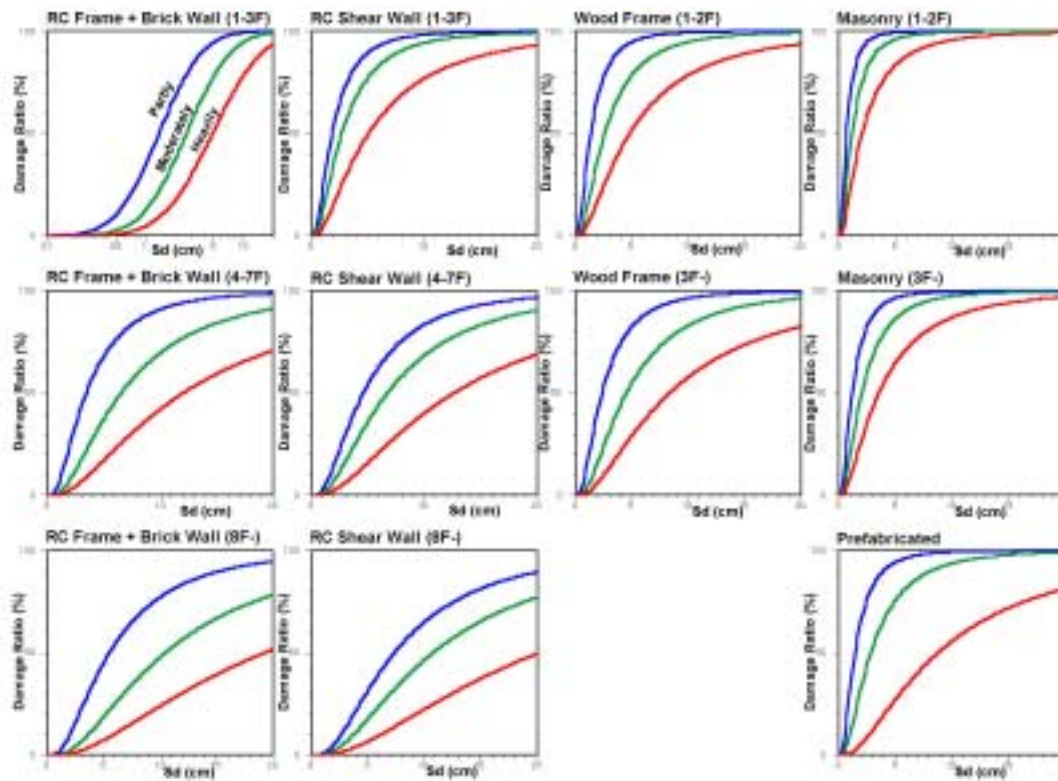

Figure 8.1.5   Fragility Function of the Buildings Constructed after 1970

8.1.2.   Seismic Motion for Damage Estimation

The building inventory database was constructed from a compilation of building census 2000 data collected for each mahalle. The data include the total number of buildings in each mahalle by the eleven structural classes that are shown in Table 8.1.1. However, seismic motion, PGA, PGV, and Sa values are calculated by 500m-grid cells. To calculate building damage by mahalle, the seismic intensity for each mahalle is necessary. If the building distribution density throughout the mahalle is not very different, it is acceptable to use the simple mean building distribution value ofseveral 500m-grid cells, which are contained either fully or partially within the mahalle boundary. However, the building distribution in Istanbul sometimes differs greatly, even within one mahalle. Therefore, the following procedure is adopted to evaluate the seismic motion by mahalle:

1) Determine the number of buildings in each 500m-grid cell using a 1/1,000 map. Developed using GIS, the IMM have a 1/1,000 map and data file that includes the location of approximately 1,000,000 buildings. The location and the number of floors for each building are included as attributes in the data file, but neither the structural type nor the constructionyear are included in this database. Therefore, this database was used only to determine the number of buildings in each 500m-grid cell.

2) Determine the number of buildings in each mahalle.

3) Calculate the seismic motion using the following formula:

$$Sm = \frac{\sum_i Sg_i \cdot Bgf_i + \sum_j Sg_j \cdot Bgp_j}{Bm}$$

Sm : seismic motion of mahalle

Sg_i : seismic motion of i - th grid

Bgf_i : number of builgings in i - th grid, which are fully included in mahalle

Bgp_j : number of buildings in the part of j - th grid that is included in mahalle,
   which are partially included in mahalle

$Bm = \sum_i Bgf_i + \sum_j Bgp_j$: building number in the mahalle

Figure 8.1.6 shows an example of seismic motion evaluation for mahalles. Figure 8.1.6 a) shows the seismic motion for each 500m-grid cell. The black lines denote the mahalle boundaries, and each black dot corresponds to an existing building. Only the southeast end of the mahalle, which is located at the center of the figure, is yellow in color, the rest is green. Therefore, the majority of buildings inthis mahalle exist in the yellow area. Figure 8.1.6b) is the seismic motion of a mahalle, which is calculated based on this procedure. The simple mean of this mahalle is green but because of the building density distribution,

this mahalle is evaluated as yellow. Determination of the seismic motion of the mahalles using this procedure leads to a better estimation of damage analysis because it reflects the building density heterogeneously.
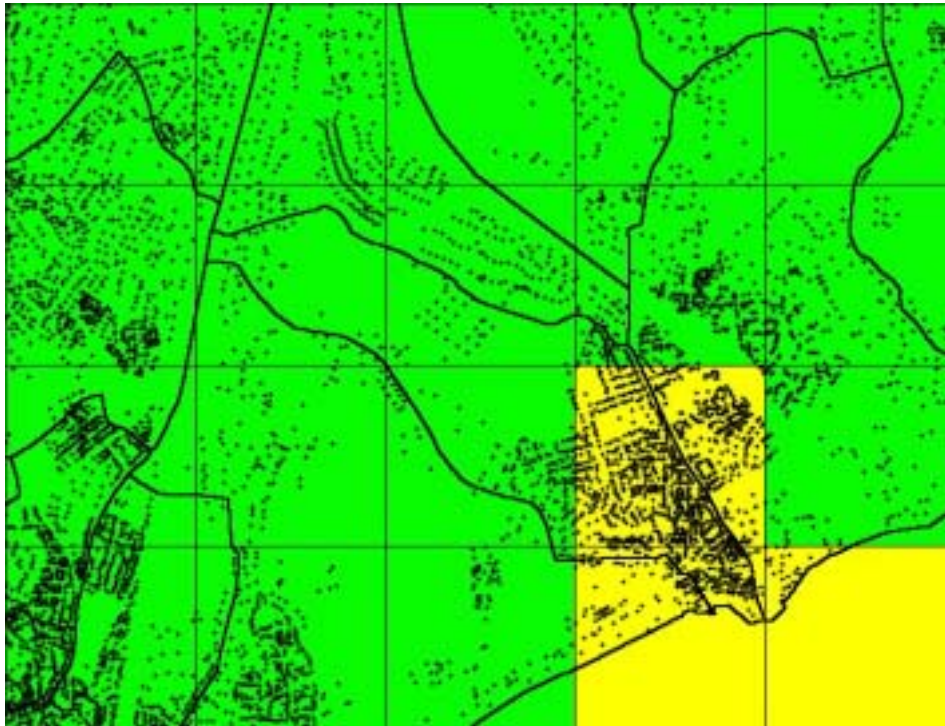
a) Seismic Motion by 500m Grid Cell
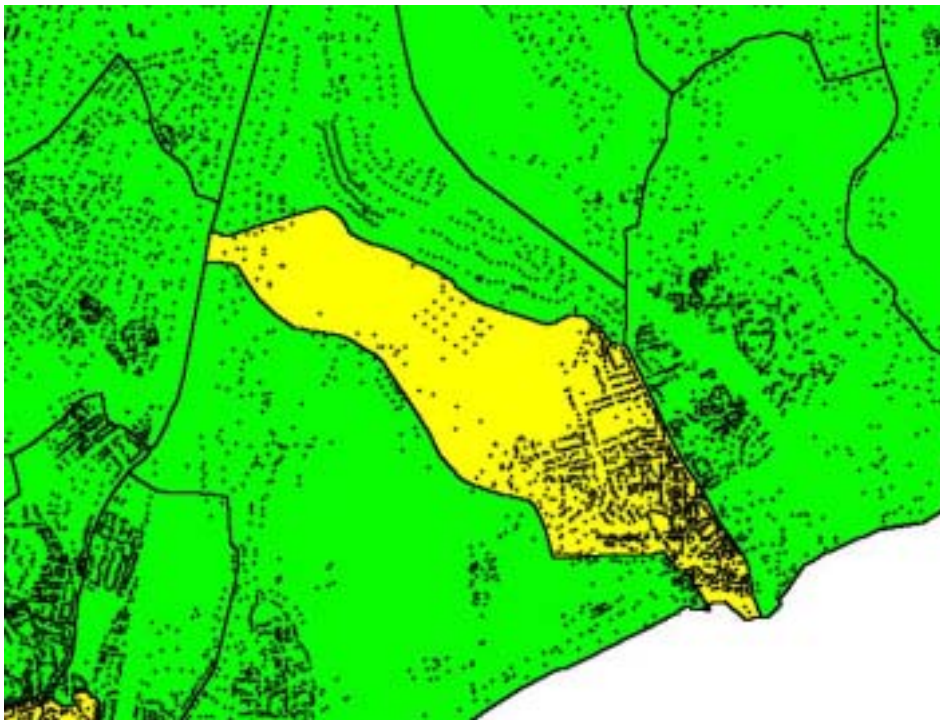
b) Seismic Motion by Mahalle for Damage Estimation

Figure 8.1.6   Example of Seismic Motion for Damage Estimation

8.1.3. Damage Estimation

Building damages are calculated based on scenario earthquakes Model A and Model C. In these estimations, every type of building included in the building census for the year 2000 is included. Important public facilities such as schools, hospitals, and fire stations will be studied separately in another chapter.

Buildings are calculated as "heavily," "moderately," or "partly" damaged. "Heavily" damaged buildings are buildings that are severely damaged or have collapsed, and these buildings are unfit to occupy until they are repaired or rebuilt. "Moderately" damaged buildings are buildings that are able to used for evacuation purposes just after the hazard, but they need to be repaired before occupied permanently. "Partly" damaged buildings can be used for living, but it is desirable they be repaired because the structure is partly damaged and its earthquake-resistance has been compromised.

The cause of damage is limited to the seismic vibration itself. Damage due to other causes, such as liquefaction, landslide, and fire are not included. This assumption will not affect the result because these phenomena are not main causes of earthquake disasters in Istanbul.

Table 8.1.2   Definition of Building Damage

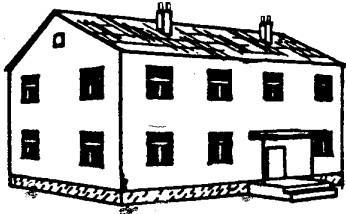| Object	All buildings in Building Census 2000	
Evaluation unit	Damage possibility of each building is evaluated and damage number in each mahalle is summed	
Cause of damage	Seismic vibration	
Definition of damage grade	Heavily	Collapse or heavy structure damage
		For evacuation: Unusable, Danger
		For living: Unusable without repair or rebuild
		(Damage Grade 4 & 5 in EMS-98; see Figure 8.1.7, Figure 8.1.8)
	Moderately	Moderate structure damage
		For evacuation: Usable
		For living: Necessary for repair
		(Damage Grade 3 in EMS-98; see Figure 8.1.7, Figure 8.1.8)
	Partly	Partly structure damage
		For evacuation: Usable
		For living: Usable, repair is desirable
		(Damage Grade 2 in EMS-98; see Figure 8.1.7, Figure 8.1.8)

Classification of damage to masonry buildings	
	Grade 1: Negligible to slight damage **(no structural damage,** **slight non-structural damage)** Hair-line cracks in very few walls. Fall of small pieces of plaster only. Fall of loose stones from upper parts of buildings in very few cases.
	Grade 2: Moderate damage **(slight structural damage, moderate** **non-structural damage)** Cracks in many walls. Fall of fairly large pieces of plaster. Partial collapse of chimneys.
	Grade 3: Substantial to heavy damage **(moderate structural damage,** **heavy non-structural damage)** Large and extensive cracks in most walls. Roof tiles detach. Chimneys fracture at the roof line; failure of individual non-structural elements (partitions, gable walls).
	Grade 4: Very heavy damage **(heavy structural damage,** **very heavy non-structural damage**) Serious failure of walls; partial structural failure of roofs and floors.
	Grade 5: Destruction **(very heavy structural damage)** Total or near total collapse.

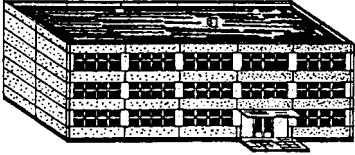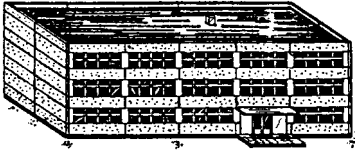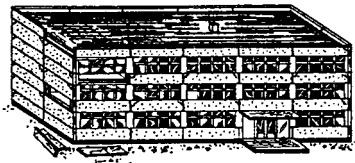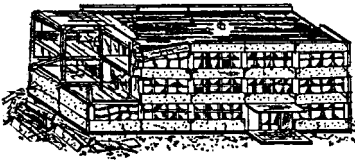**Figure 8.1.7   Classification of Damage to Masonry Building**

Source: EMS-98

Classification of damage to buildings of reinforced concrete	
	Grade 1: Negligible to slight damage **(no structural damage,** **slight non-structural damage)** Fine cracks in plaster over frame members or in walls at the base. Fine cracks in partitions and infills.
	Grade 2: Moderate damage **(slight structural damage,** **moderate non-structural damage)** Cracks in columns and beams of frames and in structural walls. Cracks in partition and infill walls; fall of brittle cladding and plaster. Falling mortar from the joints of wall panels.
	Grade 3: Substantial to heavy damage **(moderate structural damage,** **heavy non-structural damage)** Cracks in columns and beam column joints of frames at the base and at joints of coupled walls. Spalling of conrete cover, buckling of reinforced rods. Large cracks in partition and infill walls, failure of individual infill panels.
	Grade 4: Very heavy damage **(heavy structural damage,** **very heavy non-structural damage)** Large cracks in structural elements with compression failure of concrete and fracture of rebars; bond failure of beam reinforced bars; tilting of columns. Collapse of a few columns or of a single upper floor.
	Grade 5: Destruction **(very heavy structural damage)** Collapse of ground floor or parts (e. g. wings) of buildings.

Figure 8.1.8   Classification of Damage to Reinforced Concrete Buildings
Source: EMS-98

Damage is calculated for each mahalle and building classification. A summary of results is shown in Table 8.1.3. In this table, the results of a simulation of the Izmit Earthquake are also included. As building damage in some mahalle was not available, only the damage ratio is shown. The building damage analysis method is calibrated by the damage observed during the Izmit and Erzincan Earthquakes as shown in the previous section. The simulated results compare well to the observed damage.

Table 8.1.3   Summary of Building Damage

		Heavily		Heavily + Moderately		Heavily + Moderately + Partly	
Model A	Building	51,000	(7.1%)	114,000	(16%)	252,000	(35%)
	Household	216,000		503,000		1,116,000	
Model C	Building	59,000	(8.2%)	128,000	(18%)	300,000	(38%)
	Household	268,000		601,000		1,300,000	
Izmit Eq.	Simulation	(0.15%)		(0.50%)			
	Observed	(0.06%)		(0.33%)			

The damages for each district are summarized in Table 8.1.4 and Table 8.1.5. The damage for each mahalle is shown in Figure 8.1.9 and Figure 8.1.12.

Characteristics of damage for two scenario earthquakes are as follows:

(1) Model A

The total number of heavily damaged buildings is estimated as 51,000. This is 7.1% of total buildings in the Study Area. The number of moderately and heavily damaged buildings, namely the buildings that need repair in order to occupy, is 114,000. Results indicate the southern area of Istanbul is more heavily damaged than the northern area because of the earthquake motion distribution. The southern coast of the European side is the most severely affected area. More than 30% of buildings in several mahalle along the coast are heavily damaged. More than 200 buildings in several mahalle on the European side and some mahalle on the Asian side will suffer heavy damage. It should be noted that more than 300 buildings in Şilivri and Büyükçekmece are also heavily damaged.

(2) Model C

The total number of heavily damaged buildings is estimated as 59,000. This is 8.2% of the total buildings in Study Area. The number of moderately or heavily damaged buildings, namely the buildings that need to berepaired before they can be occupied, is 128,000. The damage distribution is almost the same as that of Model A. More than 40% of buildings in one mahalle along the coast of the European side are heavily damaged. More than 200 buildings in several mahalle on the European side and some mahalle on the Asian side will suffer heavy damage. It should be noted that more than 400 buildings in Şilivri and Büyükçekmece are also heavily damaged.

Figure 8.1.9   Ratio of Heavily Damaged Building : Model A

Figure 8.1.10   Ratio of Heavily Damaged Building : Model C

Figure 8.1.11   Number of Heavily Damaged Building : Model A

Figure 8.1.12   Number of Heavily Damaged Building : Model C

Table 8.1.4   Building Damage by District : Model A

District Code	District Name	Total Building Number	Heavily		Heavily + Moderately		Heavily + Moderately + Partly	
			number	%	number	%	number	%
1	Adalar	6,522	1,614	24.8	2,703	41.4	4,131	63.3
2	Avcılar	14,030	1,975	14.1	4,172	29.7	7,781	55.5
3	Bahçelievler	19,690	2,577	13.1	5,748	29.2	11,287	57.3
4	Bakırköy	10,067	1,839	18.3	3,686	36.6	6,434	63.9
5	Bağcılar	36,059	2,384	6.6	5,915	16.4	14,353	39.8
6	Beykoz	28,280	476	1.7	1,268	4.5	4,225	14.9
7	Beyoğlu	26,468	2,335	8.8	4,940	18.7	10,197	38.5
8	Beşiktaş	14,399	584	4.1	1,410	9.8	3,744	26.0
9	Büyükçekmece	3,348	351	10.5	800	23.9	1,680	50.2
10	Bayrampaşa	20,195	2,493	12.3	4,929	24.4	9,488	47.0
12	Eminönü	14,149	1,967	13.9	3,798	26.8	6,902	48.8
13	Eyüp	25,718	1,890	7.3	4,122	16.0	8,979	34.9
14	Fatih	31,947	5,111	16.0	9,908	31.0	17,689	55.4
15	Güngören	10,655	1,253	11.8	2,846	26.7	5,813	54.6
16	Gaziosmanpaşa	56,484	1,888	3.3	4,932	8.7	14,113	25.0
17	Kadıköy	38,615	1,944	5.0	4,755	12.3	12,206	31.6
18	Kartal	24,295	1,986	8.2	4,351	17.9	9,465	39.0
19	Kağıthane	28,737	1,107	3.9	2,747	9.6	7,367	25.6
20	Küçükçekmece	45,817	4,299	9.4	9,219	20.1	19,293	42.1
21	Maltepe	25,313	1,600	6.3	3,709	14.7	8,779	34.7
22	Pendik	39,877	2,835	7.1	6,365	16.0	14,343	36.0
23	Sarıyer	30,781	410	1.3	1,117	3.6	4,082	13.3
26	Şişli	22,576	727	3.2	1,874	8.3	5,386	23.9
28	Tuzla	14,727	1,331	9.0	2,844	19.3	6,024	40.9
29	Ümraniye	43,473	1,005	2.3	2,730	6.3	8,662	19.9
30	Üsküdar	43,021	1,093	2.5	2,978	6.9	9,335	21.7
32	Zeytinburnu	15,573	2,592	16.6	5,296	34.0	9,525	61.2
902	Esenler	22,700	1,355	6.0	3,312	14.6	8,216	36.2
903	Çatalca	2,573	67	2.6	176	6.8	529	20.6
904	Silivri	8,534	359	4.2	885	10.4	2,342	27.4
	Total	724,623	51,447	7.1	113,535	15.7	252,370	34.8

Table 8.1.5   Building Damage by District : Model C

District Code	District Name	Total Building Number	Heavily		Heavily + Moderately		Heavily + Moderately + Partly	
			number	%	number	%	number	%
1	Adalar	6,522	1,710	26.2	2,830	43.4	4,254	65.2
2	Avcılar	14,030	2,311	16.5	4,696	33.5	8,270	58.9
3	Bahçelievler	19,690	3,184	16.2	6,764	34.4	12,305	62.5
4	Bakırköy	10,067	2,119	21.0	4,103	40.8	6,792	67.5
5	Bağcılar	36,059	2,899	8.0	6,949	19.3	15,771	43.7
6	Beykoz	28,280	521	1.8	1,376	4.9	4,481	15.8
7	Beyoğlu	26,468	2,644	10.0	5,495	20.8	10,989	41.5
8	Beşiktaş	14,399	692	4.8	1,644	11.4	4,175	29.0
9	Büyükçekmece	3,348	415	12.4	914	27.3	1,806	53.9
10	Bayrampaşa	20,195	2,846	14.1	5,532	27.4	10,261	50.8
12	Eminönü	14,149	2,156	15.2	4,106	29.0	7,279	51.4
13	Eyüp	25,718	2,044	7.9	4,414	17.2	9,426	36.7
14	Fatih	31,947	5,776	18.1	10,996	34.4	18,900	59.2
15	Güngören	10,655	1,550	14.6	3,376	31.7	6,402	60.1
16	Gaziosmanpaşa	56,484	2,183	3.9	5,628	10.0	15,511	27.5
17	Kadıköy	38,615	2,312	6.0	5,554	14.4	13,569	35.1
18	Kartal	24,295	2,236	9.2	4,841	19.9	10,198	42.0
19	Kağıthane	28,737	1,286	4.5	3,148	11.0	8,134	28.3
20	Küçükçekmece	45,817	4,915	10.7	10,325	22.5	20,641	45.1
21	Maltepe	25,313	1,824	7.2	4,167	16.5	9,503	37.5
22	Pendik	39,877	3,128	7.8	6,956	17.4	15,263	38.3
23	Sarıyer	30,781	462	1.5	1,255	4.1	4,437	14.4
26	Şişli	22,576	884	3.9	2,232	9.9	6,093	27.0
28	Tuzla	14,727	1,456	9.9	3,079	20.9	6,344	43.1
29	Ümraniye	43,473	1,152	2.6	3,095	7.1	9,434	21.7
30	Üsküdar	43,021	1,301	3.0	3,477	8.1	10,361	24.1
32	Zeytinburnu	15,573	3,036	19.5	5,999	38.5	10,184	65.4
902	Esenler	22,700	1,655	7.3	3,922	17.3	9,111	40.1
903	Çatalca	2,573	74	2.9	194	7.5	564	21.9
904	Silivri	8,534	407	4.8	981	11.5	2,498	29.3
	Total	724,623	59,176	8.2	128,047	17.7	272,953	37.7

8.1.4. Seismic Intensity based on the Building Damage

Seismic intensity is evaluated based on building damage described in the description of the seismic intensity scale. In many microzonation studies, seismic intensity is evaluated based on the empirical relation between PGA and seismic intensity, but the definition of the seismic intensity itself is mainly associated with the degree of observed building damage. Building damage will be different depending on the building structures in an area if the PGA is the same. Therefore, it is better to estimate the seismic intensity based on building damage rather than an empirical relation between PGA and seismic intensity.

In this study, seismic intensity is not used as the index of seismic motion for the damage estimation. This is evaluated only to help enhance the understanding of engineers, who are familiar with seismic intensity.

Seismic intensity was evaluated using the European Macroseismic Scale 1998, EMS-98. In EMS-98, buildings are classified from most weak class A to class F, depending on their vulnerability. According to Erdik (2001), most buildings in Istanbul are classified as class C. Table 8.1.6shows the definition of EMS-98 for intensities VII to XI concerning building class C.

Table 8.1.6   Definition of Seismic Intensity in EMS-98

EMS-98 Intensity	Definition
XI	Most buildings of vulnerability class C suffer damage of grade 4; many of grade 5.
X	Many buildings of vulnerability class C suffer damage of grade 4; a few of grade 5
IX	Many buildings of vulnerability class C suffer damage of grade 3; a few of grade 4.
VIII	Many buildings of vulnerability class C suffer damage of grade 2; a few of grade 3.
VII	A few buildings of vulnerability class C sustain damage of grade 2.

"Few," "many," and "most" are based on a scale bar in EMS-98. In this study, ranges 0 to 15%, 15 to 55%, and 55% to 100% are used respectively"Heavily," "moderately," and "partly" damaged buildings in this study correspond to damage grade 4 and 5, 3, and 2 respectively. Based on these relations, the definition of seismic intensity is rewritten as shown in Table 8.1.7.

Table 8.1.7   Definition of Seismic Intensity in the Study

Intensity	Definition
XI:	Heavily Damage Ratio > 55%
X:	55% > Heavily Damage Ratio > 15%
IX:	15% > Heavily Damage Ratio .AND. Heavily + Moderately Ratio > 15%
VIII:	15% > Heavily + Moderately Ratio .AND. Heavily + Moderately + Partly Ratio >15%
- VII:	15% > Heavily + Moderately + Partly Ratio

The building structure composition is actually different in each mahalle, but the average composition of the Study Area is used for all mahalle as a simplification. The evaluated seismic intensity is shown in Figure 8.1.13 and Figure 8.1.14. In either Model, intensities VII to X are estimated in Istanbul. A large area of the European side is estimated to experience intensity X.

Acknowledgement

References to Section 8.1

Erdik, M., E. Durukal, Y. Biro, B. Siyahi and H. Akman, 2001, Earthquake Risk to Buildings in Istanbul and a Proposal for its Mitigation, Bogaziçı University, Kandilli Observatory and Earthquake Research Institute, Department of Earthquake Engineering, Department Report No: 2001/16,

http://www.koeri.boun.edu.tr/earthqk/earthqk.html.

European Macroseismic Scale 1998, EMS-1998,

http://www.gfz-potsdam.de/pb5/pb53/projekt/ems.

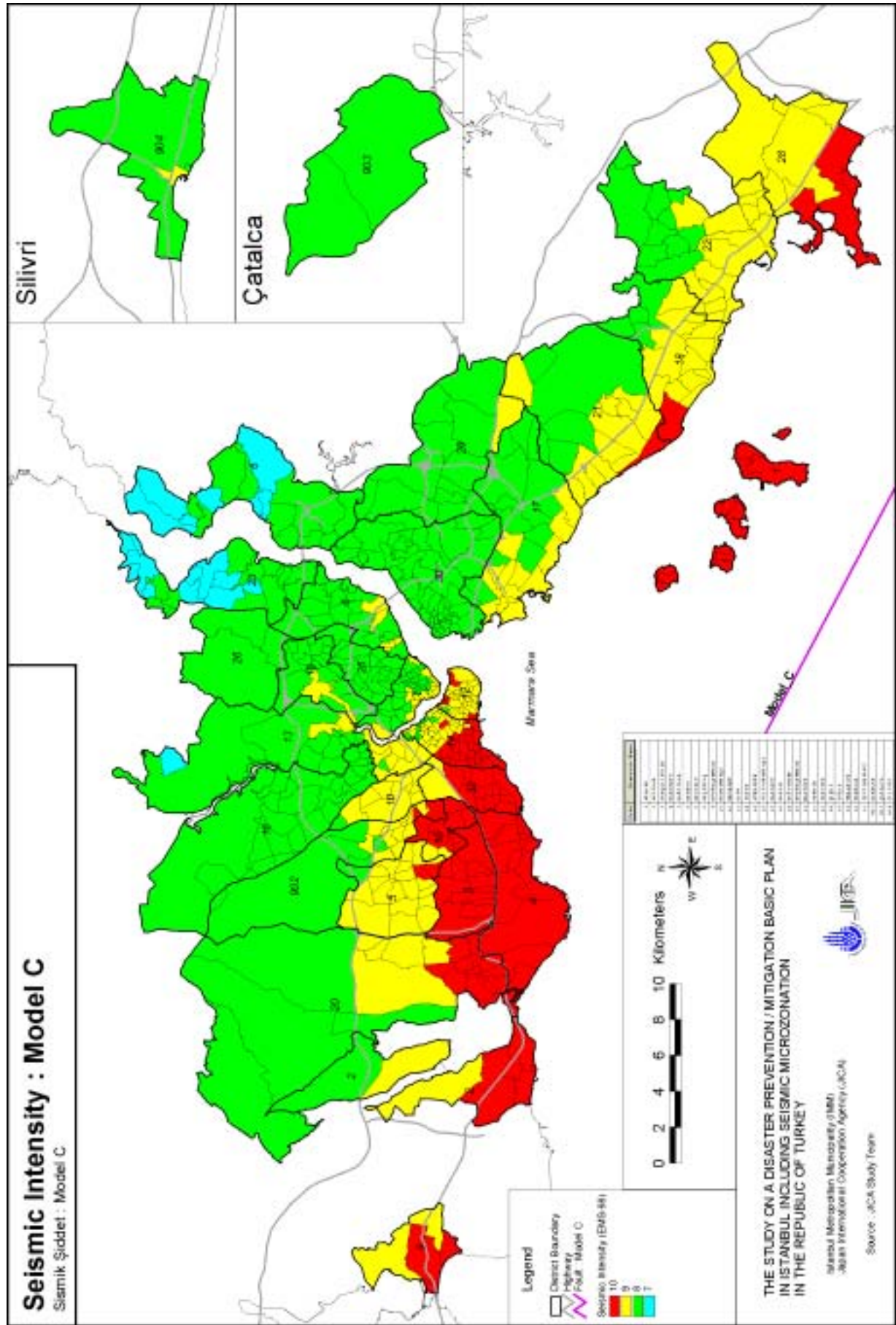**Figure 8.1.13   Seismic Intensity : Model A**

Figure 8.1.14　Seismic Intensity : Model C

8.2. Human Casualties

8.2.1. Methodology

Direct causes of earthquake casualties include collapse of buildings, fires, tsunamis, rockslides, landslides, etc. Among them, human casualties due to building collapse are a general phenomena observed in all areas subject to earthquake disasters. In Turkey, during the 1999 Izmit Earthquake, over 17,000 people were killed mainly by building collapse. Considering the weakness of buildings in Istanbul, building collapse will be the most notable cause of human casualties in future earthquakes.

Therefore, to estimate the expected number of deaths, the relation of building damage to death toll was studied based on the earthquake hazard in Turkey. Damage functions for death tolls and the number of people severely injured are derived from this analysis. Number of deaths and severe injuries is evaluated based on empirical relationships and building damage distribution. The flowchart of the human casualties estimation is shown in Figure 8.2.1.
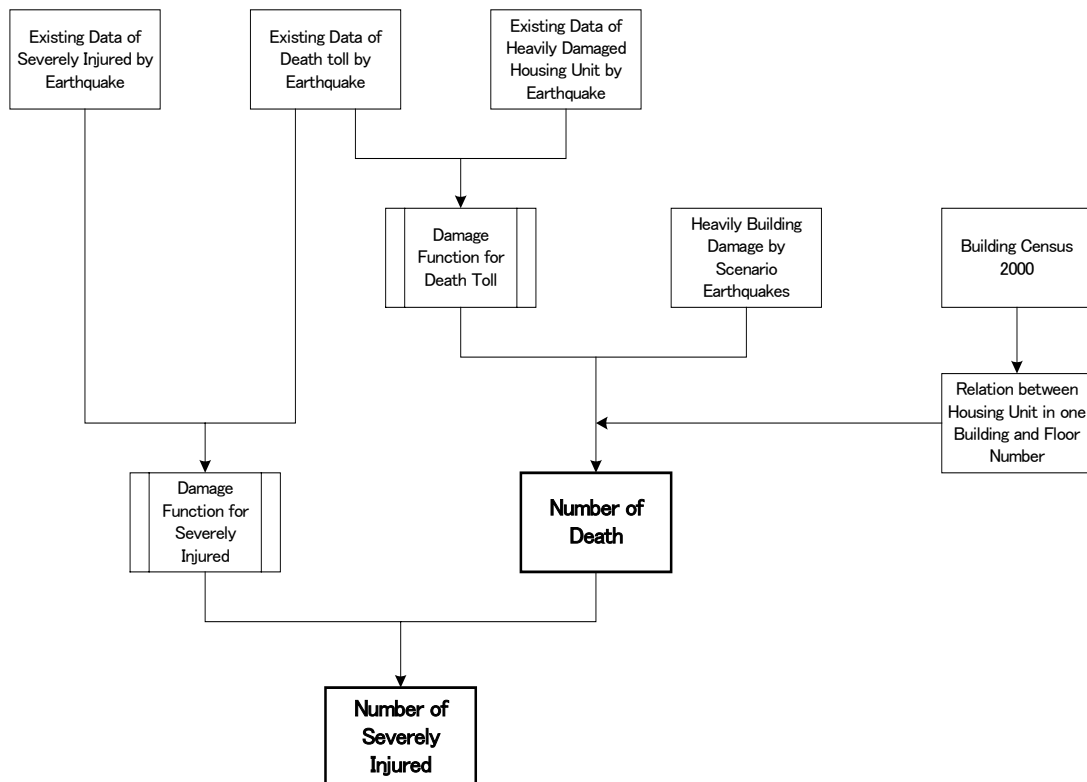

Figure 8.2.1   Flowchart of Human Casualties Estimation

Table 8.2.1 is the summary of building damage and casualties during the 1999 Izmit Earthquake in Istanbul. The damages are compiled by district. It is notable that not only is

the number of damaged buildings included in this table but also the number of damaged housing units. This data is important to evaluate the casualties in Istanbul because there are many apartment houses with many different storey heights.

To find the most appropriate indicators of death toll and building damage, several relations are examined and shown in Figure 8.2.2. For the death toll parameter, the number of deaths and death ratio are used. For the building damage parameter, the number of heavily damaged buildings, the heavily damaged building ratio, the number of heavily damaged housing units, the number of moderately to heavily damaged buildings, the ratio of moderately to heavily damaged buildings, and the number of moderately to heavily damaged housing units are used. This figure shows that the relation between the number of deaths and the number of heavily damaged housing units (upper right in Figure 8.2.2) is the most appropriate in relating the death toll to building damage.
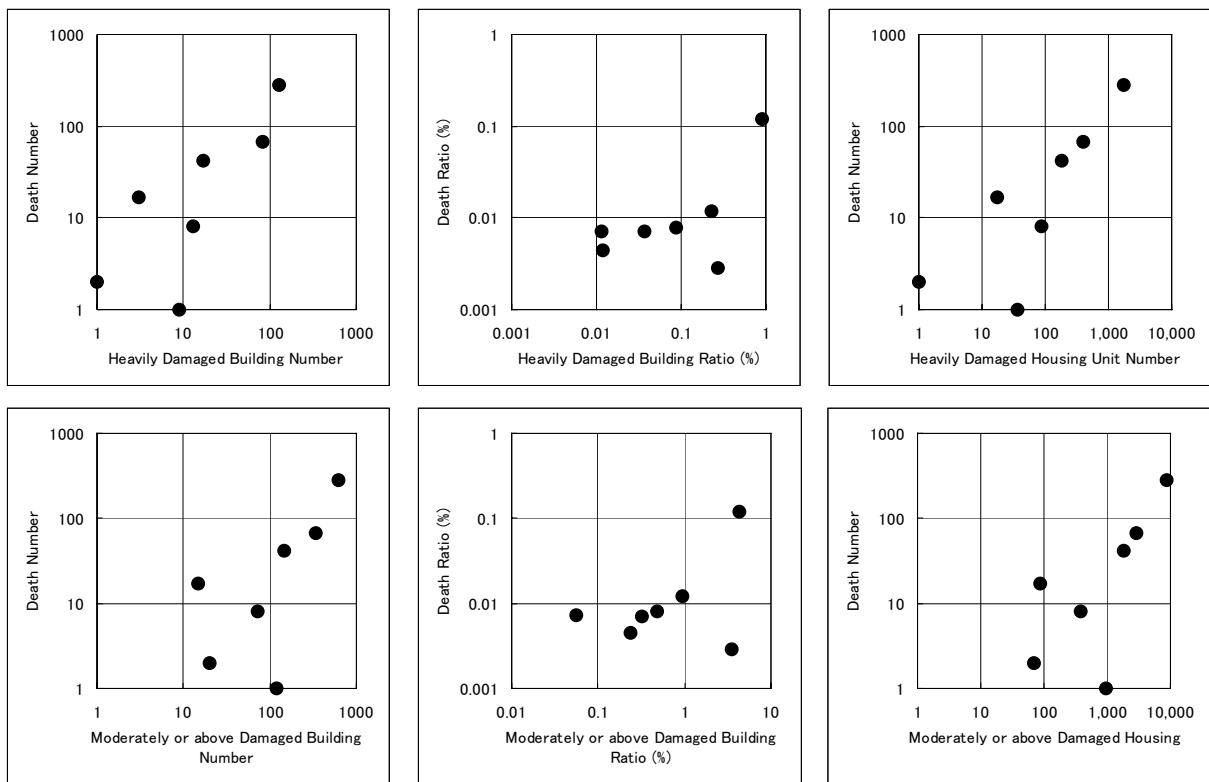

Figure 8.2.2   Several Relationships between Building Damage and Death